Thin Solid Films 517 (2009) 2936–2940

Contents lists available at ScienceDirect

Thin Solid Films

journal homepage: www.elsevier.com/locate/tsf

Competition between dislocation nucleation and void formation as the stress relaxation mechanism in passivated Cu interconnects

J. Zhang, J.Y. Zhang, G. Liu, Y. Zhao, J. Sun *

State Key Laboratory for Mechanical Behavior of Materials and School of Materials Science and Engineering, Xi'an Jiaotong University, Xi'an, 710049, China

ARTICLE INFO

Article history:
Received 6 March 2008
Received in revised form 26 November 2008
Accepted 10 December 2008
Available online 24 December 2008

Keywords:
Cu interconnects
Stress relaxation mechanisms

ABSTRACT

We perform systematic calculations to study the competition between the dislocation nucleation and void formation as stress relaxation mechanism in Cu interconnects under thermal stress, which is related to the aspect ratio (ratio of the film thickness to width) of the Cu lines. It is quantitatively found from both elastic-perfectly plastic model and kinematic strain hardening model that there exists a critical aspect ratio, below and above which the stress relaxation is dominated by the dislocation nucleation and void formation, respectively. The critical aspect ratio is revealed to modulate by both the length scale of the interconnects and the interfacial strength between the Cu lines and surroundings, suggesting potential application to achieve artificial controlling on stress relaxation mechanism in Cu lines. Calculations are in good agreement with available experiments.

1. Introduction

The reliability of Cu interconnects is a key issue in the microelectronic devices as the line width is being reduced to deep submicron scale. Due to the thermal expansion mismatch between the Cu and the surrounding materials, thermal stresses are generated in Cu lines during thermal cycling [1]. The thermal stresses can induce void formation in Cu interconnects, resulting in electrical failure. Extensive studies [2–7], both experimental and theoretical, have been performed on the stress-induced voiding in Cu interconnects, and the influences of some factors such as geometrical configuration, stress concentrations, and stress gradients have been roughly revealed. It has been found [5,6,8] that the void formation is closely dependent on the geometrical configuration of the metal lines or the ratio between height (***h***) and width (***w***), i.e., aspect ratio ***h***/***w***. In the lines with larger aspect ratio, the hydrostatic stress was higher, which causes the lines much easier to form void. As to the void location, simulations [5,6,8] clearly showed that the corners of the lines are the most favorable locations for forming voids, where the maximum hydrostatic stress gradients occurred.

Most recently, An and Ferreira [9] carried out in-situ transmission electron microscopy (TEM) observations on the microstructural evolution in 1.8 μm and 0.18 μm wide Cu interconnects under thermal stress, respectively. The Cu interconnects they used was 300 nm in thickness and 10 mm in length. The aspect ratio of interconnects is thus ***h***/***w*** = 0.167 for the 1.8 μm wide one and ***h***/***w*** = 1.67 for the 0.18 μm wide one. After thermal cycles, voids nucleation/growth was observed in the 0.18 μm wide lines while the 1.8 μm wide lines exhibited dislocation nucleation. This trend is in broad agreement with the aforementioned calculations [5,6,8] that the lines with larger ***h***/***w*** are more ready to nucleate voids. The authors attributed the dislocation nucleation in 1.8 μm wide lines to the biaxial stress condition. This means that there exist two different stress relaxation mechanisms, i.e., void formation and dislocation nucleation, in the Cu interconnects under thermal stress. Although it is qualitatively suggested that the mechanism of void formation and dislocation nucleation should dominate over the range of larger and lower ***h***/***w***, respectively, no quantitative understanding has been reported.

In this paper, we perform calculations to reveal the competition between the void formation and dislocation nucleation as stress relaxation mechanism in Cu interconnects quantitatively. Both perfect elastic-perfectly plastic model and kinematic strain hardening model are considered. A critical aspect ratio is determined to distinguish the two regions that are respectively dominated by the two stress relaxation mechanisms. The critical aspect ratio is found to be sensitive to both the length scale of interconnects (film thickness or grain size) and the Cu/surroundings interfacial strength (σ_C^*). This means that it possible to artificially modify the failure mode of Cu interconnects by controlling the interface bonding.

2. Model and simulation

2.1. Criterion for void nucleation

We first calculate the critical stress (σ_{CV}) to nucleate voids in Cu interconnects as a function of line aspect ratio. Because the void

* Corresponding author.
E-mail address: junsun@mail.xjtu.edu.cn (J. Sun).

0040-6090/$ – see front matter © 2008 Elsevier B.V. All rights reserved.
doi:10.1016/j.tsf.2008.12.031

nucleation in corners of Cu interconnects is somewhat similar to the decohesion of particle-matrix interface in inhomogeneous materials [10–15], σ_{CV} can be thus given [10,11]

$$\sigma_{CV} = \frac{\sigma_C^*}{\sqrt{f(\sigma_m/\overline{\sigma})}} \quad (1)$$

where $f(\sigma_m/\overline{\sigma})$ is the stress triaxiality level $(\sigma_m/\overline{\sigma})$ factor and can be expressed as [13]

$$f(\sigma_m/\overline{\sigma}) = \frac{2}{3}(1+\nu) + 3(1-\nu)(\sigma_m/\overline{\sigma})^2 \quad (2)$$

where the hydrostatic stress, σ_m, and the effective stress, $\overline{\sigma}$, are defined as $\sigma_m = (\sigma_x+\sigma_y+\sigma_z)/3$ and $\overline{\sigma} = \sqrt{\frac{1}{2}\left((\sigma_x-\sigma_y)^2+(\sigma_x-\sigma_z)^2+(\sigma_y-\sigma_z)^2\right)}$, respectively, and ν is Poisson's ratio. As well known, the total stress of an element of material could be divided into two parts, i.e., hydrostatic stress and deviatoric stress, that due to change in volume and that due to change in shape, respectively. Because of the requirement of mass conservation, the volume expansion usually induces voids in the material. Hydrostatic stress is thus known as the driving force for stress voiding, or in the more strict sense, driving force for stress void nucleation. The von-Mises stress, which is usually used as a criterion for plastic deformation, is in a form of octahedral shear stress that does not include the hydrostatic stress components and usually does not affect the volumetric changes of material. The ratio between σ_m and $\overline{\sigma}$, i.e., the stress triaxiality level of $\sigma_m/\overline{\sigma}$, reflects the assemble constraint. The fracture is always initiated at the zone with maximum value of the stress triaxiality because the separation of materials, i.e., cavity nucleation and development, occurs most easily within the zone due to maximum volume dilatation of materials caused by the maximum $\sigma_m/\overline{\sigma}$ [10]. That is, voiding occurs at larger $\sigma_m/\overline{\sigma}$ or higher constraint while shear deformation at stress-state of lower constraint, resulting in the cavitating and ductile deformation of the materials, respectively. The stress triaxiality level or $\sigma_m/\overline{\sigma}$ thus reflects the relative possibility of the two different fracture/deformation modes [10–13]. As to the devices in the microelectronics fields, low constraint is desirable because it will cause plastic deformation rather than catastrophic void formation. From above equations, one can see that the critical stress to nucleate voids in Cu lines depends not only on the stress condition or stress triaxiality level but also on the Cu/surroundings interfacial strength σ_C^*. The stress triaxiality level is closely influenced by the aspect ratio of the lines, which can be quantitatively calculated using finite element methods as treated in previous investigations [4–6,8,10–13].

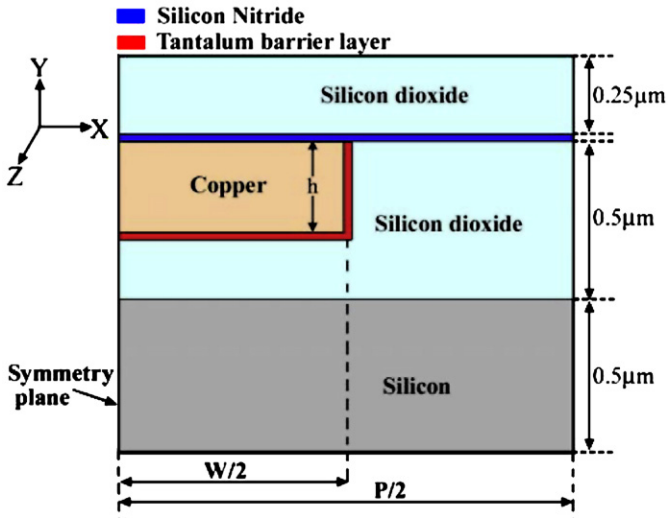

Fig. 1. Schematic showing the half of cross section of a periodic unit cell of a passivated Cu interconnects.

Table 1
Parameters used in present calculations [16–19]

Material	Property			
	E (*GPa*)	ν	α ($10^{-6}/K$)	σ_y (*MPa*)
SiO_2	59	0.16	1	
Ta	185.7	0.342	6.5	
SiN	220.8	0.27	3.2	
Si	130	0.28	$1.296+4.156\times10^{-3}\,T$	
Cu	$145.94-4.153\times10^{-2}\,T$	0.33	$14.25+7.275\times10^{-3}\,T$	$730.6-1.054\,T$

The strain hardening rate $H = 77$ GPa for kinematic strain hardening model.

2.2. Finite element model

For calculation purpose, the geometrical model of Cu lines is typically shown in Fig. 1, where half the cross-section of a periodic unit cell of the Cu interconnect structure is presented. This system consists of a 0.3 μm thick Cu interconnect on a 0.2 μm thick F-doped SiO_2 on a 0.5 μm thick Si substrate, with the interconnect passivated 0.25 μm thick layer of SiO_2 on an etch stop layer (SiN_x) of thickness 50 nm, tantalum (Ta) barrier layer of thickness 20 nm for the bottom and 10 nm for the sidewall. These thicknesses are held constant during studying the effect of aspect ratio scaling. The unit cell has half width, *p/2*, which is assumed to be twice that of half width of Cu interconnect, *w/2*, in all calculations. The choice of 0.5 μm for Si substrate thickness is to reduce calculations in the finite element simulation. Although the Si substrate used in practice has a thickness thicker than 0.5 μm, it was found from our pre-simulations that the results are slightly dependent on the Si substrate thickness, mainly due to the assumption of constraint at the base of the Si substrate. Therefore, a reduced thickness for the Si substrate is reasonable and favorable in the simulations.

In present work, the directions along the line-width, interconnect thickness, and interconnect length are defined by the *x*, *y* and *z* directions, respectively. The interconnect is assumed to be very long and has both ends connected to other structures. Hence it experiences no strain in the *z* direction. Thus, a plane strain condition is used. Due to the symmetry, only the right half of the unit segment is simulated. The left side is the yz symmetry plane such that no displacement is allowed in *x* direction. The Si substrate is constrained at its base, i.e. no y displacement. Along the right side wall ($x = p/2$), no displacement is allowed in *x* direction. This preserves the periodic natures of the line structures in the *x* direction. The top surface is free to move during deformation. Si, SiO_2, SiN_x and Ta are characterized as isotropic linear elastic solid, while Cu is characterized as either isotropic elastic-perfectly plastic [5,6] or kinematic strain hardening [19]. In other words, both isotropic elastic-perfectly plastic model and kinematic strain hardening model are employed for the Cu interconnects in order to achieve more comprehensive understanding. The details about the kinematic strain hardening model can be referred to Ref. [19], and the strain hardening rate *H* is also evaluated as 77 GPa after Ref. [19]. Some other material properties [16–19] used for simulation are list in Table 1.

Calculations are carried out for cooling from the initial stress-free temperature at 673 K to room temperature at 298 K. The commercial Ansys finite element software is used to calculate the stresses. Both mean stresses and stress distributions are obtained after calculations. The mean stresses are averaged over the cross-sectional area of the Cu lines, and the stress triaxiality level is defined as $\sigma_m/\overline{\sigma}$. The hydrostatic stress gradient is the ratio of the difference between the stress values of two consecutive nodes to the distance between the nodes. The magnitude of the hydrostatic gradient, $|\nabla\sigma_{HS}|$, is defined as $\sqrt{\left(\frac{d\sigma_{HS}}{dx}\right)^2+\left(\frac{d\sigma_{HS}}{dx}\right)^2}$. The mean stresses will be used to ascertain the stress relaxation mechanism, void formation or dislocation nucleation, of the whole Cu interconnects and the hydrostatic gradient will be used to show where is the best place for void formation, if the stress

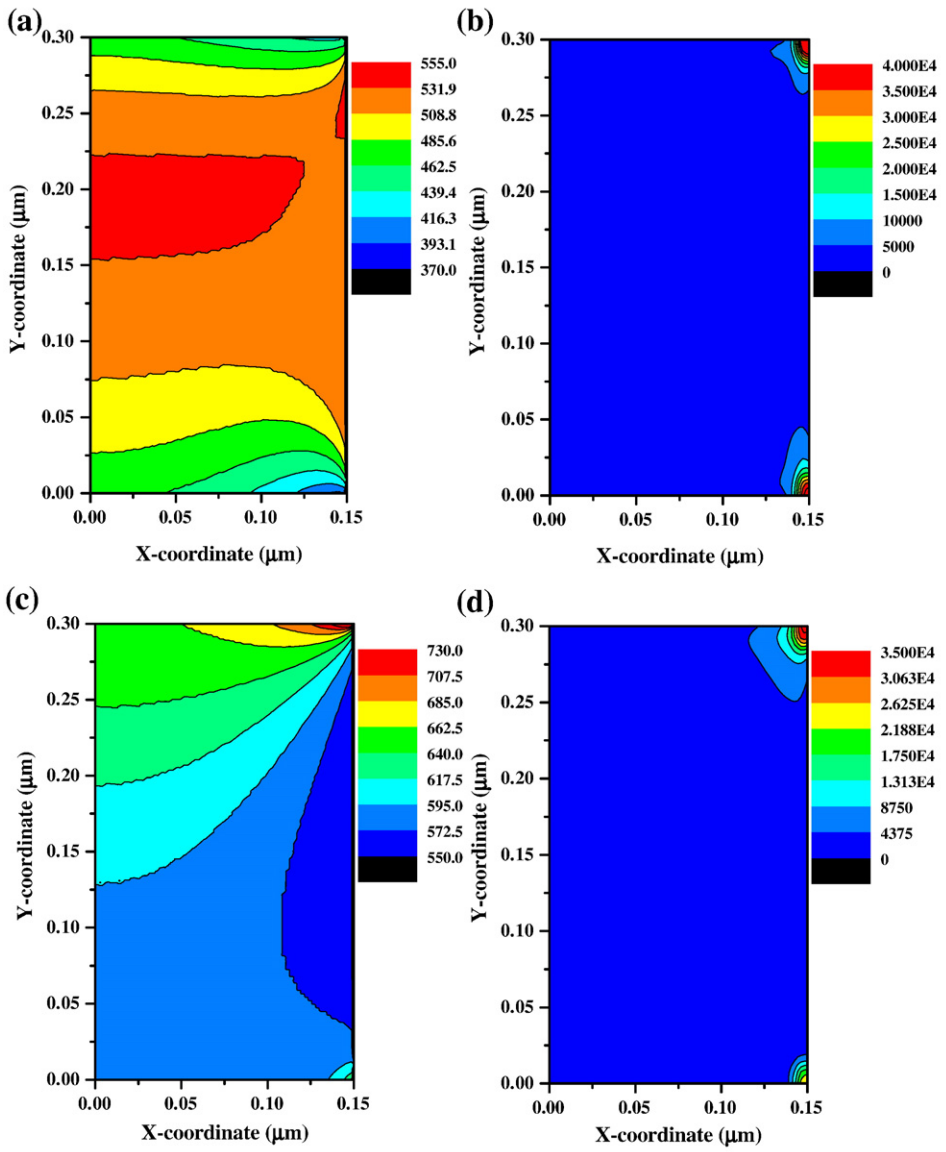

Fig. 2. Hydrostatic stress distribution (a and c) and hydrostatic stress gradient contours (b and d) in Cu interconnects with aspect ratio of 1. (a) and (b) are from the elastic-perfectly plastic model while (c) and (d) from kinematic strain hardening model.

relaxation mechanism is the void formation. We will address these two important issues in the following section.

3. Results and discussions

3.1. Hydrostatic stress gradient and the voiding location

Fig. 2 typically shows the hydrostatic stress (a and c) and hydrostatic stress gradient (b and d) contours in the Cu interconnect with aspect ratio of 1, calculated from both the elastic-perfectly plastic model (a and b) and the kinematic strain hardening model (c and d), respectively. In elastic-perfectly plastic model, the highest hydrostatic stress region is at the centre of interconnect (Fig. 2 a) while the maximum hydrostatic stress gradient is located at interconnect corner (Fig. 2 b). These results agree well with Ang's results [5,6]. On the other hand, both the highest hydrostatic stress and the maximum hydrostatic stress gradient are at the interconnect corner in kinematic strain hardening model (see Fig. 2 c and d). It has been found that the hydrostatic stress gradient is better to predict a void location than hydrostatic stress [5]. Present results from both models, i.e., the maximum stress gradient at the corner of interconnects, indicate that the voids are prone to appear at the corners, in good agreement with experimental observations [9].

However, local stress distribution and stress gradient cannot be used to make sure whether the relaxation mechanism of the Cu interconnects should be void formation or dislocation nucleation. Dislocation nucleation is dependent not only on the stress conditions but also on the characteristic length (*e.g.*, grain size, width, thickness) of the Cu interconnects. The characteristic length of the Cu interconnects is a parameter of the whole interconnects, which indicates that the critical stress for dislocation nucleation should be also an averaged stress over the whole interconnects. In this consideration, averaged stresses will be mostly used in following discussions to reveal the competitive effect between the dislocation nucleation and the void formation as stress relaxation mechanism.

3.2. Competition between the void formation and the dislocation nucleation

The calculated average hydrostatic stress and stress triaxiality level in the periodically arranged Cu lines are shown in Figs. 3 and 4, respectively, as a function of line aspect ratio ***h*/*w***. In Fig. 3, the

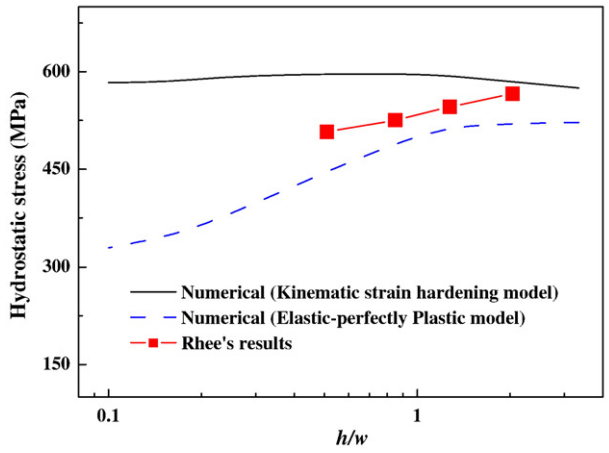

Fig. 3. Dependence of hydrostatic stress on aspect ratio of Cu interconnects (lines), predicted by using elastic-perfectly plastic model and kinematic strain hardening model, respectively. The experimental results from Rhee's [20] are also shown for comparison (dots).

hydrostatic stress from elastic-perfectly plastic model is found to increase monotonically with increasing line aspect ratio in the range of $\boldsymbol{h}/\boldsymbol{w}<3$, in broad agreement with the available experimental results from Rhee et al. [20]. No maximum hydrostatic stresses exist at aspect ratio of about 1 because the line structures studied here are periodic parallel lines [8] rather than single line. The hydrostatic stress from kinematic strain hardening model, however, is not very sensitive to the line aspect ratio and is larger than that from elastic-perfectly plastic model. The experimental results [20] are reasonably located between the calculations from the two models. In Fig. 4, the calculations on stress triaxiality level are presented as lines (left *y*-axis). The solid line and dash line are the results from the kinematic strain hardening model and the elastic-perfectly plastic model, respectively. Both models predict a monotonic increase in stress triaxiality level with increasing the line aspect ratio, while the elastic-perfectly plastic model yields larger results than those from the kinematic strain hardening model.

Fig. 5 (a) and (b) shows the dependence of σ_{CV} on aspect ratio of lines as a function of the Cu/surroundings interface strength σ_C^* (σ_C^* could be given ~90 MPa [21], Here, σ_C^*=70, 90, and 110 MPa are respectively assumed), predicted using the elastic-perfectly plastic model and the kinematic strain hardening model, respectively. Two conclusions can be drawn from Fig. 5 (a) and (b). The one is that the

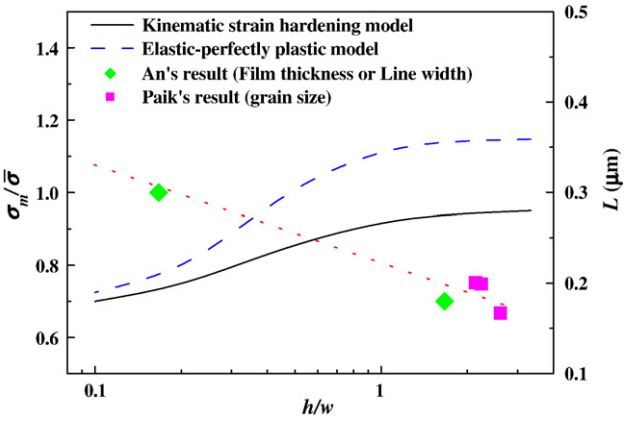

Fig. 4. Dependence of stress triaxiality level on aspect ratio of Cu interconnects (left *Y*-axis) (lines), predicted by using elastic-perfectly plastic model and kinematic strain hardening model, respectively. Some experimental results [10,26] are presented in this figure to show the dependence of *L* on aspect ratio (right *Y*-axis) (dots).

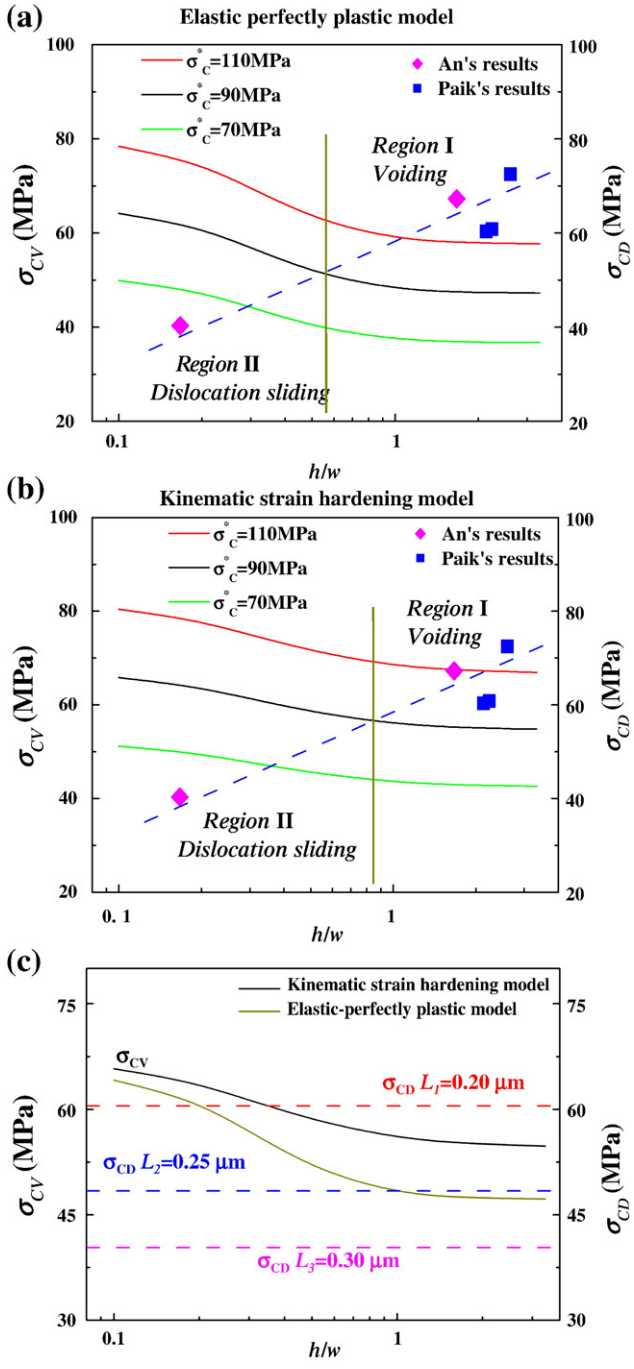

Fig. 5. Calculated critical stress for void formation σ_{CV} (left *Y*-axis, solid lines) and critical stress for dislocation formation (right *Y*-axis, dots) in Cu interconnects as a function of line aspect ratio. The intersecting point corresponds to the critical aspect ratio: line width-dependent *L* is considered using the experimental result [10,26] as shown in Fig. 3, (a) and (b) correspond to the calculations from elastic-perfectly plastic model and kinematic strain hardening model, respectively; (c) line width-independent *L* is considered and *L*=0.20, 0.25, and 0.30 μm are assumed respectively. σ_C^* is estimated 90 MPa to calculate σ_{CV}.

larger is lower $\boldsymbol{h}/\boldsymbol{w}$ the higher is σ_{CV}, which indicates that the lines with large aspect ratio are most likely to undergo voiding [22]. The other one is that σ_{CV} is strongly dependent on σ_C^* and weak interface bonding will reduce the critical stress to nucleate voids significantly.

When $\boldsymbol{h}/\boldsymbol{w}$ is reduced and it is difficult to form voids (larger σ_{CV}), dislocation nucleation is then an alternative mechanism to relax the thermal stress. In the metal films or interconnects, dislocation activity should be constrained by the dimension of materials and the

dislocations are much easier to nucleate as increasing grain size or sample size [23–25]. Some reports (e.g., [26]) showed that, in metal interconnects, the grain size increases with widening the lines even at the same thickness, see dots in Fig. 4 from Paik et al.'s experiments [26]. Paik et al. [26] found that, with the increase in line width of the 470 nm-thick Cu lines from 0.18 μm (aspect ratio=2.61) to 0.21 μm (aspect ratio=2.24) and to 0.22 μm (aspect ratio=2.13), the average grain size raises from 167 nm to 199 nm and to 201 nm, correspondingly. This indicates that, at wider $\boldsymbol{w}$ or lower $\boldsymbol{h}/\boldsymbol{w}$ and stress triaxiality level, it is possible to nucleate the dislocations as stress relaxation mechanism rather than to form voids at higher stress triaxiality level.

The critical stress for dislocation nucleation can be expressed as [25]

$$\sigma_{CD} = \frac{Gb}{L} \tag{3}$$

where G=48.4 GPa and b=0.25 nm are shear modulus and Buregers vector of Cu, respectively, L is the length scale of the Cu films (the lowest of either the film thickness $\boldsymbol{h}$ or the grain size d). This critical stress σ_{CD} can be thus calculated as a function of L or $\boldsymbol{h}/\boldsymbol{w}$ by using the experiments results in Fig. 4. The calculated σ_{CD} is depicted in Fig. 5 (a) and (b) as dots to compare with σ_{CV}. One can find that the dependence of σ_{CD} on $\boldsymbol{h}/\boldsymbol{w}$ is contrary to that of σ_{CV}. σ_{CV}, as mentioned above, monotonically increases with reducing $\boldsymbol{h}/\boldsymbol{w}$. However, σ_{CD} monotonically decreases with reducing $\boldsymbol{h}/\boldsymbol{w}$. Of especial interest to note is that the σ_{CD} vs $\boldsymbol{h}/\boldsymbol{w}$ curve intersects with the σ_{CV} vs $\boldsymbol{h}/\boldsymbol{w}$ curves, making two regions clearly divided by a critical aspect ratio. One region, defined region I, is dominated by void formation at higher aspect ratio, where the required stress to nucleate voids is lower than that to nucleate dislocations. The other region, defined region II, is dominated by dislocation nucleation at lower aspect ratio, where it is more difficult to form voids due to lower stress triaxiality level. The competition between the dislocation nucleation and the void formation as stress relaxation mechanism results in the formation of the two regions marked by the critical aspect ratio.

From Fig. 5 (a) and (b), we can quantitatively explain the experimental results of An et al. [9] in a clear and direct way. The Cu lines with $\boldsymbol{h}/\boldsymbol{w}$=0.167 and 1.67 fall in region II and region I, respectively, indicating dislocation nucleation is easer to happen in the former while void formation in the latter. These are in good agreement with An et al.'s experiments.

It should be especially addressed that the critical aspect ratio, as revealed from Fig. 5 (a) and (b), is dependent strongly on the interfacial strength σ_C^*. Larger σ_C^* will yield a larger critical aspect ratio. For example, when σ_C^* increases from 70 MPa to 90 MPa, the corresponding critical aspect ratio for elastic-perfectly plastic model will enhance from about 0.3 up to about 0.6. This indicates that the competition between the dislocation nucleation and void formation can be modulated by the interfacial strength and it is possible to tailor the stress relaxation mechanism artificially by controlling the interfacial strength, which may be helpful to the material design for next generation Cu interconnects.

In above calculations, line width-dependent grain size is considered according to previous experiments. Without loss of generality, L is further assumed to be independent of line width. Similarly, two regions are still clearly distinguished, divided by the intersecting point or critical aspect ratio, as shown in Fig. 5 (c) where σ_{CD} is a constant regardless of $\boldsymbol{h}/\boldsymbol{w}$ because L does not change with $\boldsymbol{h}/\boldsymbol{w}$. Three values are assumed for L, i.e., L=0.20, 0.25, and 0.30 μm, respectively, and one can see from Fig. 5 (c) that the critical aspect ratio of the Cu lines is also dependent on L. The larger is L, the larger is the critical aspect ratio. This means that the stress relaxation mechanism in the Cu interconnects should be remarkably controlled by the length scale or by the geometrical length of film thickness as well as the microstructural length of grain size.

Finally, it should be especially noted that, if low-k materials are used as the interlevel dielectric (ILD) materials instead of SiO_2, the stress relaxation behaviors will be much different from present predictions. This is mainly because the thermal stresses in the Cu interconnects depend remarkably on the thermal–mechanical properties of the used ILD materials [18]. Low-k materials have a much lower elastic modulus and a higher thermal expansion coefficient than SiO_2, which will induce a much different hydrostatic stress and concomitant constraint effect. Compared with SiO_2, if the Low-k materials have a thermal expansion coefficient more close to that of the Cu, the constraint effect on Cu interconnects will be reduced and thus the dislocation nucleation will be promoted to be the dominant stress relaxation mechanism. This will be helpful to avoid the catastrophic failure of forming voids in the Cu interconnects.

4. Conclusions

In summary, we perform systematic calculations on the competition between the dislocation nucleation and void formation as stress relaxation mechanism in Cu interconnects under thermal stress. From both elastic-perfectly plastic model and kinematic strain hardening model, the mechanism of dislocation nucleation and void formation is quantitatively predicted to dominate in the range of lower and higher aspect ratio, respectively, divided clearly by a critical aspect ratio. The critical aspect ratio is revealed to modulate by both the length scale of the Cu lines and the Cu/surroundings interfacial strength. Calculations are in good agreement with available experiments.

The present results suggest an application potential to achieve artificial controlling on stress relaxation mechanism in Cu lines. In order to avoid the formation of voids, the Cu interconnects with low aspect ratio (thin film thickness or large width) are preferred. Besides, using softer materials in the stack instead of SiO_2 can also promote the dislocation nucleation, reducing the voiding.

Acknowledgements

This work was supported by the National Basic Research Program of China (Grant No. 2004CB619303), the National Natural Science Foundation of China. This work was also supported by the 111 Project of China under Grant No. B06025.

References

[1] Z. Suo, Reliability of Interconnects Structures, Elsevier Science Ltd., 2003.
[2] P. Borgesen, J.K. Lee, R. Gleixner, C.Y. Li, Appl. Phys. Lett. 60 (1992) 1706.
[3] J.A. Nucci, Appl. Phys. Lett. 66 (1995) 3585.
[4] W. Shao, Z.H. Gan, Thin Solid Films 504 (2006) 298.
[5] D. Ang, R.V. Ramanujan, Mater. Sci. Eng. A423 (2006) 157.
[6] D. Ang, C.C. Wong, R.V. Ramanujan, Thin Solid Films 515 (2007) 3246.
[7] D.W. Gan, G.T. Wang, P.S. Ho, X. Morrow, J.P. Leu, 5th Annual International Interconnect Technology Conference, Proceedings of the IEEE 2002 International Interconnect Technology Conference, Burlingame, U.S.A., June 3–5, 2002, p. 271.
[8] Y.L. Shen, J. Appl. Phys. 82 (1997) 1578.
[9] J.H. An, P.J. Ferreira, Appl. Phys. Lett. 89 (2006) 151919.
[10] J. Sun, Eng. Fract. Mech. 44 (1993) 789.
[11] J. Sun, Z.J. Deng, Z.H. Li, Int. J. Fract. 42 (1990) R39.
[12] J. Sun, Eng. Fract. Mech. 39 (1991) 799.
[13] J. Sun, Z.J. Deng, Z.H. Li, M.J. Tu, Eng. Fracture. Mech. 34 (1989).
[14] G. Liu, J. Sun, C.W. Nan, K.H. Chen, Acta. Mater. 53 (2005) 3459.
[15] G. Liu, G.J. Zhang, R.H. Wang, W. Hu, J. Sun, K.H. Chen, Acta. Mater. 55 (2007) 273.
[16] R.E. Jones Jr., M.L. Basehore, Appl. Phys. Lett. 50 (1987) 725.
[17] T. Marieb, A.S. Mack, N. Cox, D. Gardner, X.C. Mu, in: H.J. Frost, M.A. Parker, C.A. Ross, E.A. Holm (Eds.), Conference on Polycrystalline Thin Films – Structure, Texture, Properties, and Applications II, Boston, U.S.A., November 27–December 1, 1995, Polycrystalline Thin Films: Structure, Texture, Properties, and Applications II, vol. 403, 1995, p. 639.
[18] J.M. Paik, H. Park, Y.C. Joo, Microelectron. Eng. 71 (2004) 348.
[19] Y.L. Shen, J. Vac. Sci. Technol. B. 21 (2003) 1258.
[20] S.H. Rhee, Y. Du, P.S. Ho, J. Appl. Phys. 93 (2003) 3926.
[21] T. Kitamura, H. Hirakata, D.V. Truong, Thin Solid Films. 515 (2007) 3005.
[22] P.A. Flinn, Mater. Res. Bull. 20 (1995) 70.
[23] E. Arzt, Acta. Mater. 46 (1998) 5611.
[24] G.P. Zhang, C.A. Volkert, R. Schwaiger, P. Wellner, E. Arzt, O. Kraft, Acta. Mater. 54 (2006) 3127.
[25] B.Von. Blanckenhagen, P. Gumbsch, E. Arzt, Phil. Mag. Lett. 83 (2003) 1.
[26] J.M. Paik, I.M. Park, Y.C. Joo, K.C. Park, J. Appl. Phys. 99 (2006) 024509.